WMAP constraints on scalar-tensor cosmology and the variation of the gravitational constant

Ryo Nagata,[1,2,*] Takeshi Chiba,[2] and Naoshi Sugiyama[1]

[1]*Division of Theoretical Astrophysics, National Astronomical Observatory, 2-21-1, Osawa,*
Mitaka, Tokyo 181-8588, Japan
[2] *Department of Physics, Kyoto University, Kyoto 606-8502, Japan*
(Dated: February 2, 2008)

We present observational constraints on a scalar-tensor gravity theory by χ^2 test for CMB anisotropy spectrum. We compare the WMAP temperature power spectrum with the harmonic attractor model, in which the scalar field has its harmonic effective potential with curvature β in the Einstein conformal frame and the theory relaxes toward Einstein gravity with time. We found that the present value of the scalar coupling, i.e. the present level of deviation from Einstein gravity (α_0^2), is bounded to be smaller than $5 \times 10^{-4-7\beta}$ (2σ), and $10^{-2-7\beta}$ (4σ) for $0 < \beta < 0.45$. This constraint is much stronger than the bound from the solar system experiments for large β models, i.e., $\beta > 0.2$ and 0.3 in 2σ and 4σ limits, respectively. Furthermore, within the framework of this model, the variation of the gravitational constant at the recombination epoch is constrained as $|G(z = z_{rec}) - G_0|/G_0 < 0.05(2\sigma)$, and $0.23(4\sigma)$.

PACS numbers: 98.65.Dx ; 98.80.Es ; 04.80.Cc

I. INTRODUCTION

The discovery of acoustic peaks on the anisotropy spectrum of the cosmic microwave background (CMB) opened the way to measure the early universe. The high quality data recently provided by the Wilkinson Microwave Anisotropy Probe (WMAP) mission [1] makes such a challenge feasible. The measurement of the characteristic length of various processes at the recombination epoch reveals the physical process in the early universe [2]. Length scales, which exhibit in the angular spectrum of the CMB as a characteristic feature, depend on the horizon length which is controlled by gravity. Usually, the horizon length at the recombination epoch is a function of the amount of non-relativistic matter. The strength of gravity caused by matter and radiation determines how much time consumed to make the universe cool enough to recombine hydrogens. However, the strength of gravity depends not only on the amount of matter but also on the coupling strength of gravitational interaction. Thus the CMB anisotropy spectrum contains the information about the magnitude of the gravitational constant at the recombination epoch.

Constancy of physical "constants" is the fundamental issue which has long history and has attracted much interest [3]. The recent attempts toward unifying all elementary forces [4] predict the existence of scalar fields whose vacuum expectation values determine the physical "constants". In such context, scalar-tensor gravity theories, whose original version was proposed by Jordan [5] and Brans and Dicke [6] and were extended in a more general framework later [7], are the most promising candidates among the alternatives of Einstein gravity. In scalar-tensor theories, the coupling of a massless scalar field to the Ricci scalar provides a natural framework of realizing the time-variation of the gravitational constant via the dynamics of the scalar field.

In the Jordan-Brans-Dicke theory [5, 6] (hereafter, we refer to it as the Brans-Dicke theory for simplicity) which is the simplest example of scalar-tensor theories, a constant coupling parameter ω is introduced. In the limit $\omega \to \infty$, the gravitational constant can not change and Einstein gravity is recovered. Although scalar-tensor theories including the Brans-Dicke theory are compatible with the Einstein gravity in several aspects, they have many deviations from it. Weak-field experimental tests in solar-system have constrained the post-Newtonian deviation from the Einstein gravity, $\omega > 500$ [8, 9, 10, 11]. According to some recent reports, this bound would be updated to several thousands [12, 13, 14]. Such a small deviation implies that the variability of the background scalar field is also small.

In more general scalar-tensor theories with non-trivial coupling functions $\omega(\phi)$, the small deviation is not the outcome of fine-tuning because the cosmological evolution drives ω toward infinity in the late cosmological epochs and naturally reduces the present observable effects of ϕ field [15]. If such attractor mechanism takes place, the nature of gravity (the variability of the background scalar field, weak-field deviations, etc.) can be significantly different in the early universe. Hence, information on the different cosmological epochs may constrain such theories. A simple and natural extension of the Brans-Dicke theory to the attractor model is the harmonic attractor model in which the scalar field has a quadratic effective potential of a positive curvature in the Einstein conformal frame. The analysis of big-bang nucleosynthesis (BBN) in the harmonic attractor model [16] restricts two parameters characterizing the potential (its curvature β and today's gradient α_0). It is concluded

that the BBN limit on the possible deviation from Einstein gravity ($2\omega_0 + 3 = \alpha_0^{-2}$) is much stronger than the present observational limits in large $\beta(> 0.3)$ models. We can extract the information about the early universe also by the analysis of structure formation [17]. The advantage of the use of the CMB fluctuations is that the physics of CMB is well understood and that we now have very accurate observational data. The trace of primordial fluctuation can be seen clearly in the CMB anisotropy spectrum where the information on the early universe up to the last scattering time is projected on the acoustic peaks [18, 19, 20].

We compare the CMB temperature anisotropy spectrum measured by WMAP with that in the scalar-tensor cosmological model mentioned above. The formulations of background and perturbation equations and the detailed explanation of physical processes can be found in our previous paper [20]. The purpose of this work is to constrain the deviation of the scalar-tensor gravity from the Einstein gravity and to find, in the framework of this model, how large the variation of the gravitational constant is allowed.

This paper is organized as follows: In Section II, the scalar-tensor cosmological model and its observational consequences are explained. In Section III, we describe the overview of our analysis for constraining the scalar-tensor coupling parameters. In Section IV, the models are compared with the WMAP data and the result of χ^2 test is presented. Finally, some conclusions are in Section V.

II. MODEL AND ITS PREDICTIONS

The action describing a general massless scalar-tensor theory is

$$S = \frac{1}{16\pi G_0} \int d^4x \sqrt{-g} \left[\phi R - \frac{\omega(\phi)}{\phi}(\nabla\phi)^2 \right] + S_m[\psi, g_{\mu\nu}], \quad (1)$$

where G_0 is the Newtonian gravitational constant measured today, and $\omega(\phi)$ is the dimensionless coupling parameter of the nonminimal coupling which is a function of ϕ. The last term in Eq.(1) denotes the action of matter which is a functional the matter variable ψ and the metric $g_{\mu\nu}$. The deviation from the Einstein gravity depends on the asymptotic value of ϕ field at spatial infinity. According to the cosmological attractor scenario [15], the dynamics of the cosmological background ϕ field is analogous to that of a particle damping its motion toward the minimum of an external potential in the Einstein conformal frame. As the generic feature of a potential near a minimum is parabolic, we shall study the case where the potential is quadratic. This setup corresponds to $\omega(\phi)$ of the following form,

$$2\omega(\phi) + 3 = \left\{ \alpha_0^2 - \beta\ln(\phi/\phi_0) \right\}^{-1}, \quad (2)$$

where ϕ_0, α_0 and β are the present value of background ϕ field, today's potential gradient and curvature, respectively. We consider non-negative value of β since curvature near a minimum is positive. If $\beta = 0$, this model is reduced to the Brans-Dicke theory. Moreover, the model with $\alpha_0 \to 0$ and $\beta = 0$ is the Einstein gravity. In the first post-Newtonian approximation, deviations from general relativity are proportional to the well-known Eddington (PPN) parameters as,

$$\gamma_{\text{Edd}} - 1 = -2\alpha_0^2/(1 + \alpha_0^2), \quad (3)$$

$$\beta_{\text{Edd}} - 1 = \frac{1}{2}\beta\alpha_0^2/(1 + \alpha_0^2)^2. \quad (4)$$

We see explicitly from Eqs. (3) and (4) that post-Newtonian deviations from general relativity tend to zero with α_0 at least as fast as α_0^2. This holds true for weak-field deviations of arbitrary post-Newtonian order [21]. One of the most stringent empirical limits for PPN parameters is

$$-1.7 \times 10^{-3} < 4\beta_{\text{Edd}} - \gamma_{\text{Edd}} - 3 < 1.5 \times 10^{-4} \ (1\sigma), (5)$$

which is obtained by the Lunar Laser Ranging experiment [22]. In the framework of the present model, this translates into

$$\alpha_0^2 < 1.5 \times 10^{-4}/(\beta + 1). \quad (6)$$

The cosmological evolution equations based on the theory are

$$\rho' = -3\frac{a'}{a}(\rho + p), \quad (7)$$

$$\left(\frac{a'}{a}\right)^2 = \frac{8\pi G_0 \rho a^2}{3\phi} - \frac{a'}{a}\frac{\phi'}{\phi} + \frac{\omega}{6}\left(\frac{\phi'}{\phi}\right)^2, \quad (8)$$

$$\phi'' + 2\frac{a'}{a}\phi' = \frac{1}{2\omega + 3}\left\{ 8\pi G_0 a^2(\rho - 3p) - \phi'^2\frac{d\omega}{d\phi} \right\}. \quad (9)$$

A flat universe is assumed here. The prime denotes a derivative with respect to the conformal time. ρ and p are the total energy density and pressure, respectively. The effective gravitational constant measured by Cavendish-type experiments is given by [10, 23]

$$G(\phi) = \frac{G_0}{\phi}\frac{2\omega(\phi) + 4}{2\omega(\phi) + 3}. \quad (10)$$

The requirement that today's gravitational constant be in agreement with the Newton's constant determines the present value of ϕ as

$$\phi_0 = \frac{4 + 2\omega_0}{3 + 2\omega_0} = 1 + \alpha_0^2, \quad (11)$$

where ω_0 denotes the present value of $\omega(\phi)$. The system of perturbation equations is found in ref.[20].

Fig.1 shows the examples of typical ϕ evolution. ϕ is frozen during the radiation-dominated epoch and begins to grow at the matter-radiation equality time to realize the Newtonian gravitational constant at present. As
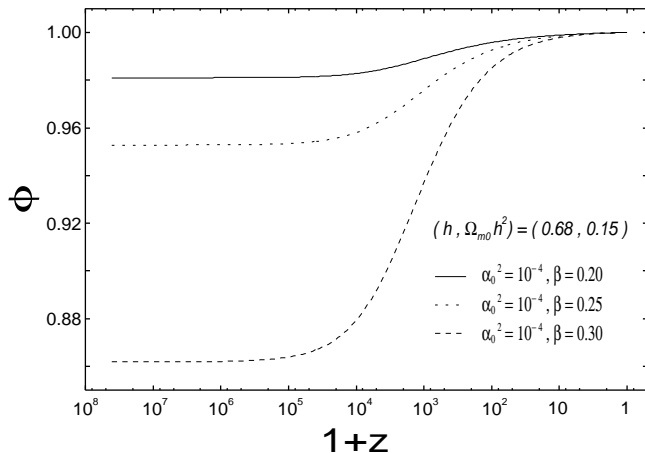
FIG. 1: The typical time evolution of ϕ in the scalar-tensor models with ΛCDM parameters. The smaller ϕ in the early epochs results in the smaller horizon length than that in the Einstein model.

FIG. 2: The typical CMB temperature anisotropy spectra in the scalar-tensor models with ΛCDM parameters. Also the WMAP data is displayed for reference. The normalizations are marginalized to the WMAP data. The acoustic peak locations are shifted to smaller angular scales due to the smaller sound horizon length (cf. Fig.1).

ϕ moves upward, $2\omega + 3$ increases toward infinity, and therefore the present small deviation from the Einstein gravity is naturally realized. The increase of $2\omega + 3$ decelerates the motion of ϕ and finally ϕ converges to some value which corresponds to the minimum of the effective potential. As increasing α_0 or β, we obtain smaller initial ϕ. This results in the smaller horizon length in the early epochs, which leaves distinct traces on the CMB spectrum.

The typical CMB anisotropy spectra are shown in Fig.2. The locations of acoustic peaks (sound horizon scale) and that of diffusion damping tail are dependent on the horizon length at the recombination epoch. Since the matching condition of ϕ_0 restricts the deviation of the present horizon length from that in the Einstein gravity, these angular scales directly represent the horizon length at recombination. Therefore, the shift of these angular scales to smaller scales is due to the large gravitational constant at recombination. The locations of acoustic peaks are shifted to smaller angular scales in proportion to the horizon length. Although the diffusion tail is also moved to smaller scale, it has weaker dependence on the horizon length, and hence the width between the first peak and the diffusion tail becomes thinner, which results in the suppression of small scale peaks. The motion of ϕ field and its fluctuation also distorts the spectrum. Roughly speaking, they make the first acoustic peak more prominent than higher peaks [20]. However this effect is not so significant compared with the effect of changing Ω_{m0} or Ω_{b0}.

III. METHOD

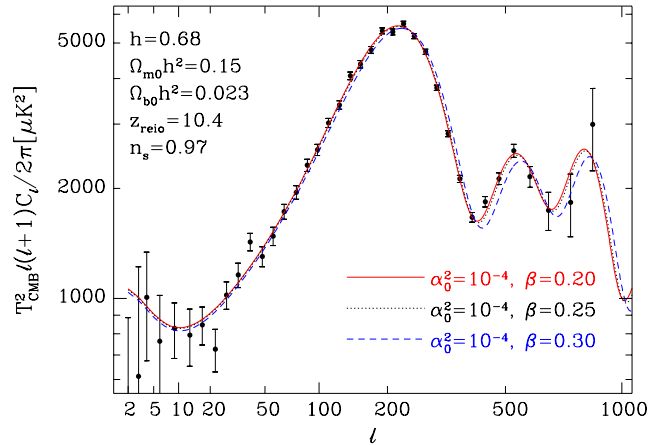Let us describe the overview of our analysis. To constrain the scalar-tensor coupling parameters, we compare the models to the WMAP temperature anisotropy spectrum [24] adopting the routine provided by the authors of ref.[25] to compute the values of χ^2. We employ a cosmological constant (Λ) which is the simplest dark energy model that can account for the late time cosmic acceleration.

In the model concerned in this paper, the CMB spectrum depends on the three classes of model parameters. The first class consists of the conventional background cosmological parameters which are today's Hubble parameter (h), today's non-relativistic matter content (Ω_{m0}), today's baryon content (Ω_{b0}), the redshift of cosmic reionization (z_{reio}), today's CMB temperature (T_{CMB}), the helium mass fraction (Y_{He}), and the neutrino effective number (N_ν). We restrict ourselves to flat space models and hence today's amount of dark energy, which is introduced as a component of total energy and whose equation of state is $p_\Lambda/\rho_\Lambda = -1$, is a function of Ω_{m0} so that the modified Friedmann equation (Eq.(8)) is satisfied. The second class consists of perturbation parameters characterizing the origin of fluctuations. They are the combination of adiabatic and isocurvature initial perturbations, the scalar spectral index (n_s) and the overall normalization (A). The last class consists of the scalar-tensor coupling parameters which are the present deviation from the Einstein gravity ($\alpha_0{}^2$) and the curvature (β) of the harmonic effective potential in the Einstein conformal frame.

For the cosmological parameters, we use the following priors that are principally based on the WMAP 68% mean confidence range. Hubble parameter (h) takes the value between 0.67 and 0.77. As described in the next section, larger Ω_{m0} (smaller cosmological constant) shifts the acoustic peak locations to larger angular scales also in the scalar-tensor models. Therefore we allow

the non-relativistic matter of somewhat large content, $\Omega_{m0} \in (0.10, 0.78)$, to confirm how small the value of χ^2 for a set of $(\alpha_0{}^2, \beta)$ can be at its minimum. Similarly, the range of today's baryon content is set as $\Omega_{b0} \in (0.023, 0.055)$. We employ instantaneous reionization at the redshift (z_{reio}) between 12 and 22. We set the CMB temperature as $T_{CMB} = 2.726K$ from $COBE$ [26] and the neutrino effective number (N_ν) is fixed at 3.04. Although the helium mass fraction depends on the result of BBN, which is dependent on other parameters, it does not significantly affect the CMB spectrum. Therefore we set it as $Y_{He} = 0.24$.

According to the studies devoted to the generation of fluctuations during particular inflation models with scalar-tensor gravity [27, 28, 29], it is found that, although isocurvature perturbations could be produced during scalar-tensor inflation, they are in general negligible compared with adiabatic perturbations and then the spectrum of the initial perturbations is not precisely scale invariant. Hence we employ adiabatic initial condition and allow the scalar spectral index to take the slightly deviated value from scale invariant one as follows: $n_s \in (0.95, 1.03)$. As the overall normalization for each model, we survey the region between 0.8 and 2.2 in unit of $COBE$ normalization factor.

Since we are interested in setting a constraint from CMB alone, we survey the ranges of α_0 and β including the regions which have been ruled out by the solar constraint shown in Eq.(6) as

$$\alpha_0{}^2 \in (4 \times 10^{-8}, 4 \times 10^{-2}), \quad (12)$$
$$\beta \in (0, 0.45). \quad (13)$$

These regions roughly correspond to $10 < \omega_0 < 10^7$ from Eq.(2).

IV. COMPARISON WITH OBSERVATIONS

In this section, we show the result of χ^2 test comparing the harmonic attractor model with the WMAP data.

In Fig.3, we show the χ^2 contour map on $\alpha_0{}^2 - \beta$ plane, marginalizing over the other parameters. We find that the scalar-tensor coupling parameters are constrained as

$$\alpha_0{}^2 < 5 \times 10^{-4-7\beta} \quad (2\sigma), \quad (14)$$
$$\alpha_0{}^2 < 10^{-2-7\beta} \quad (4\sigma). \quad (15)$$

The contour map in Fig.3 has a sharp edge approximately on the curve, $\alpha_0^2 = 10^{-2-7\beta}$. Beyond this curve, χ^2 of the models rapidly increases and then those models are statistically improbable to explain the observed spectrum.

Next, we consider the variation of the gravitational constant at the recombination epoch. In Fig.4, we show the χ^2 for the gravitational constant at the recombination epoch ($G_{rec} = G(\phi_{rec})$), marginalizing over other parameters. Here, ϕ_{rec} is the value of ϕ at the recombination epoch. We find that the deviation of the gravitational

constant from today's value is constrained as

$$|G_{rec} - G_0|/G_0 < 0.05 \quad (2\sigma), \quad (16)$$
$$|G_{rec} - G_0|/G_0 < 0.23 \quad (4\sigma). \quad (17)$$

The deviation of the gravitational constant from today's value up to 5 % does not significantly change χ^2 and the degree of fit of such models is comparable to that of WMAP team's best fit model, while even larger deviation increases χ^2. In the models on the curve, the locations of acoustic peaks are fitted to those of the observed spectrum and then, in order to pull back the peaks shifted by the larger gravitational constant to observed locations, Ω_{m0} and Ω_{b0} are out of their favorable values to fit the shape of the spectrum. The χ^2 for the gravitational constant at our initial time ($G_{ini} = G(\phi_{ini})$) is also displayed for reference. Here, ϕ_{ini} is the value of ϕ at $z_{ini}(\sim 10^8)$. We find that the CMB constraint on the gravitational constant at z_{ini}, $|G_{ini} - G_0|/G_0 < 0.12$, is on the same order as the BBN bound [30]: $0.7 < G_{BBN}/G_0 < 1.4(2\sigma)$, and it can be comparable to the BBN bound on the harmonic model Eq.(2) [16] since our analysis is limited to $\beta < 0.45$.

In Fig.5, we show the allowed post-Newtonian deviations at three different epochs. The curve for today's deviation parameter ($\alpha_0{}^2$) is identical to the cross section of the contour map at $\beta = 0$ and hence it is identical to the χ^2 curve for the Brans-Dicke models. The sharp edge mentioned above is located around $\alpha_0{}^2 \sim 10^{-2}(\omega_0 \sim 50)$. The models whose Brans-Dicke parameter is much smaller than the lower bound by the solar system experiments can be compatible with CMB fluctuation, which was expected previously. Even if we require that the degree of fit should be comparable to that of WMAP team's best fit model, the boundary of the corresponding region is still beyond the solar bound. On the other hand, the deviation at the recombination epoch and z_{ini} are relatively loosely constrained: $\alpha_{rec}{}^2 = 1/(2\omega(\phi_{rec}) + 3) < 7 \times 10^{-2}, \alpha_{ini}{}^2 = 1/(2\omega(\phi_{ini}) + 3) < 2 \times 10^{-1}(4\sigma)$. This might have implications for extended inflation scenarios [31]-[34].

In Figs.6 and 7, we plot the χ^2 for Ω_{m0} and Ω_{b0}, marginalizing over other parameters. Compared with the Einstein models, the scalar-tensor models can be more probable in high density models because the scalar-tensor models have the two more tunable parameters to fit acoustic peak locations. Although the peak locations are dependent on baryon abundance, large amount of non-relativistic matter results in very low peak heights which cannot be compensated by baryon drag especially on the 2nd peak. On the other hand, in low Ω_{b0} models, there is no definite difference between the scalar-tensor and the Einstein models. The observed spectrum have the prominent peaks and hence low density and small baryon abundance models are not so ill-fitted compared with the scalar-tensor models within the surveyed parameter range.

Finally, we comment on the case if we allow non-flat universe models. Even in the case of non-flat models,
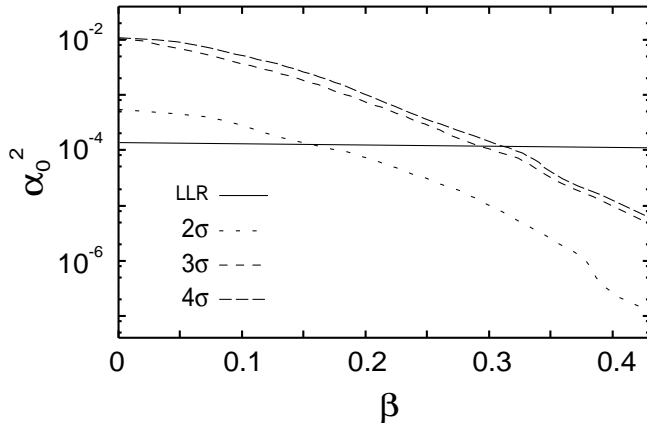
FIG. 3: The χ^2 contour map on $\alpha_0{}^2 - \beta$ plane for the scalar-tensor ΛCDM models, where the other parameters are marginalized. Also the solar bound from the LLR experiment is shown for reference. Note that the horizontal axis $\alpha_0{}^2$ is almost proportional to $\gamma_{Edd} - 1$ from Eq.(3). There exists a sharp edge approximately on the curve, $\alpha_0^2 = 10^{-2-7\beta}$. Beyond the curve, χ^2 of the models rapidly increases. Although, in the figure, the boundary curves only up to 4σ level are drawn, χ^2 continues to inflate for larger coupling parameters.

the constraint for the scalar-tensor coupling parameters $(\alpha_0{}^2, \beta)$ of Eq.(15) would not significantly change because the value of ϕ in the early epochs depends on these parameters exponentially. On the other hand, the constraint for the gravitational constant at the recombination epoch would become much weaker because acoustic peak locations can be easily modulated in curved models without disturbing CDM or baryon abundance significantly. This degeneracy would be improved by observations at even smaller scales uncovering the diffusion cut-off [35] because the diffusion length depends on horizon length in a different way from peak locations. The ratio of the angular scale of the sound horizon to that of the diffusion scale is independent of projection effect, and hence it can provide the information on the horizon length at the recombination epoch.

V. CONCLUSION

In this paper, we have quantitatively compared the CMB temperature spectrum in the scalar-tensor flat ΛCDM model to the WMAP data by χ^2 test of goodness of fit.

The present deviation from the Einstein gravity (α_0^2) must be smaller than $5 \times 10^{-4-7\beta}$ (2σ), and $10^{-2-7\beta}$ (4σ) for $0 < \beta < 0.45$. This constraint is much stronger than the bound from the solar system experiments for large β models, i.e., $\beta > 0.2$ and 0.3 in 2σ and 4σ limits, respectively. Within the framework of the harmonic attractor model, the difference between the gravitational constant at the recombination epoch and at the present is constrained as $|G(z = z_{rec}) - G_0|/G_0 < 0.05(2\sigma)$ and
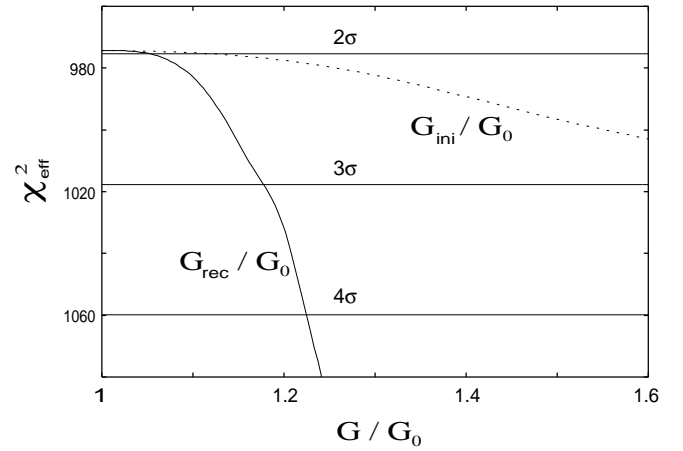

FIG. 4: The χ^2 for the scalar-tensor ΛCDM models as a function of G_{rec} and G_{ini}, where the other parameters are marginalized. The degree of freedom $\nu(= \sigma^2/2)$ is 891.
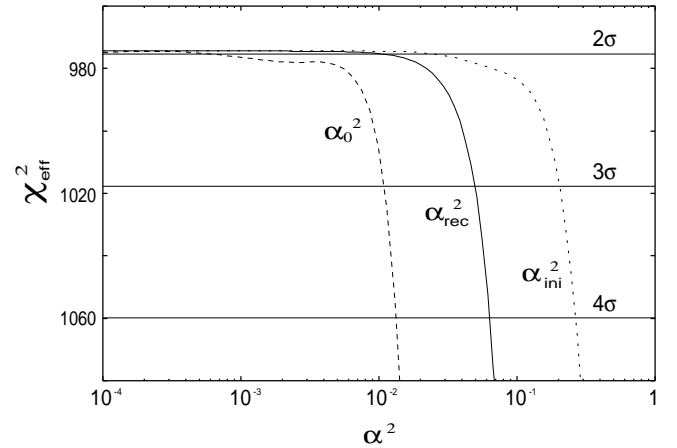

FIG. 5: The χ^2 for the scalar-tensor ΛCDM models as a function of $\alpha_0{}^2, \alpha_{rec}{}^2$ and $\alpha_{ini}{}^2$, where the other parameters are marginalized. The curve for $\alpha_0{}^2$ is idential to the χ^2 for the Brans-Dicke models. The degree of freedom $\nu(= \sigma^2/2)$ is 891.

$0.23(4\sigma)$. This is the first-time bound on the variation of the gravitational constant from CMB anisotropy spectrum. While the present deviation from the Einstein gravity is severely constrained $(\alpha_0^2 < 10^{-4})$, larger deviation during radiation dominated epochs is compatible with CMB. Indeed $\alpha_{ini}{}^2$ up to 2×10^{-2} can be within 2σ level. Although our analysis is limited to flat models, the further small scale CMB anisotropy data which will be provided in future [35] would break the degeneracy and would significantly improve the bound.
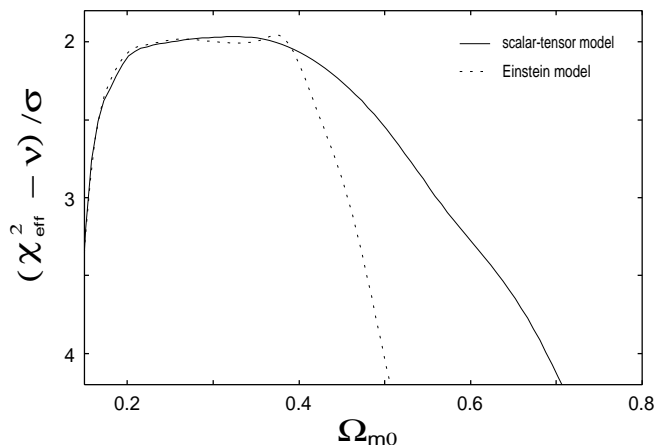
FIG. 6: The χ^2 for the Einstein and the scalar-tensor ΛCDM models as a function of Ω_{m0}, where the other parameters are marginalized. $\nu(=\sigma^2/2)$ in the scalar-tensor and the Einstein models are 891 and 893, respectively.
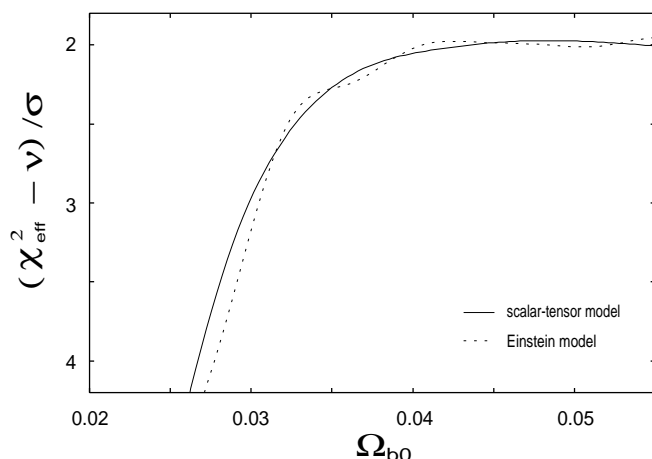

FIG. 7: The χ^2 for the Einstein and the scalar-tensor ΛCDM models as a function of Ω_{b0}, where the other parameters are marginalized. $\nu(=\sigma^2/2)$ in the scalar-tensor and the Einstein models are 891 and 893, respectively.

[1] C.L. Bennett et al., [WMAP collaboration], astro-ph/0302207.
[2] W. Hu, N. Sugiyama, and J. Silk, Nature **386** 37 (1997).
[3] T. Chiba, arXiv:gr-qc/0110118; J. P. Uzan, Rev. Mod. Phys. **75**, 403 (2003).
[4] M. B. Green, J. H. Schwarz, and E. Witten, *Superstring Theory* (Cambridge University Press, Cambridge, 1987).
[5] P. Jordan, Nature (London) **164**, 637 (1949); *Schwerkraft und Weltall* (Vieweg, Braunschweig, 1955); Z. Phys. **157**, 112 (1959).
[6] C. Brans and R. H. Dicke, Phys. Rev. **124**, 925 (1961); R.H.Dicke, *ibid.* **125**, 2163 (1962); **152**, 1 (1968).
[7] P. G. Bergmann, Int. J. Theor. Phys. **1**, 25 (1968); R. V. Wagoner, Phys. Rev. D **1**, 3209 (1970).
[8] R. D. Reasenberg *et al.*, Astrophys. J. **234**, L219 (1979).
[9] D. S. Robertson, W. E. Carter and W. H. Dillinger, Nature **349**, 768 (1991).
[10] C. M. Will, *Theory and Experiment in Gravitational Physics* (Rev.Ed., Cambridge University Press, Cambridge, 1993).
[11] D. E. Lebach, B. E. Corey, I. I. Shapiro, M. I. Ratner, J. C. Webber, A. E. E. Rogers, J. L. Davis, and T. A. Herring, Phys. Rev. Lett. **75**, 1439 (1995).
[12] T. M. Eubanks, J. O. Martin, B. A. Archinal, F. J. Josties, S. A. Klioner, S. Shapiro, and I. I. Shapiro, *Advances in solar system tests of gravity* (ftp://casa.usno.navy.mil/navnet/postscript/prd_15.ps).
[13] C. M. Will, Living Rev. Relativ. **4**, 4 (2001).
[14] J. D. Anderson, E. L. Lau, and G. Giampieri, arXiv:gr-qc/0308010.

[15] T. Damour and K. Nordtvedt, Phys. Rev. Lett. **70**, 2217 (1993); Phys. Rev. D **48**, 3436 (1993).

[16] T. Damour and B. Pichon, Phys. Rev. D **59**, 123502 (1999).

[17] A. R. Liddle, A. Mazumdar and J. D. Barrow, Phys. Rev. D **58**, 027302 (1998).

[18] X. Chen and M. Kamionkowski, Phys. Rev. D **60**, 104036 (1999).

[19] F. Perrotta, C. Baccigalupi, and S. Matarrese, Phys. Rev. D **61**, 023507 (2000); C. Baccigalupi, S. Matarrese, and F. Perrotta, Phys. Rev. D **62**, 123510 (2000).

[20] R. Nagata, T. Chiba, and N. Sugiyama, Phys. Rev. D **66**, 103510 (2002).

[21] T. Damour and G. Esposito-Farèse, Phys. Rev. D **53**, 5541 (1996).

[22] J. G. Williams, X. X. Newhall, and J. O. Dickey, Phys. Rev. D **53**, 6730 (1996).

[23] T. Damour and G. Esposite-Farése, Class. Quantum Grav. **9**, 2093 (1992).

[24] G. Hinshaw et al., [WMAP collaboration], astro-ph/0302217.

[25] L. Verde et al., [WMAP collaboration], astro-ph/0302218.

[26] J. C. Mather, D. J. Fixsen, R. A. Shafer, C. Mosier, and D. T. Wilkinson, Astrophys. J. **512**, 511 (1999).

[27] A. A. Starobinsky and J. Yokoyama, arXiv:gr-qc/9502002.

[28] J. Garcia-Bellido and D. Wands, Phys. Rev. D **52**, 6739 (1995).

[29] T. Chiba, N. Sugiyama, and J. Yokoyama, Nucl. Phys. B **530**, 304 (1998).

[30] F.S. Accetta, L.M. Krauss and P. Romanelli, Phys. Lett. B **248**, 146 (1990).

[31] D. La and P. J. Steinhardt, Phys. Rev. Lett. **62**, 376 (1989); Phys. Lett. B **220**, 375 (1989).

[32] E. J. Weinberg, Phys. Rev. D **40**, 3950 (1989); D. La, P. J. Steinhardt, and E. W. Bertschinger, Phys. Lett. B **231**, 231 (1989).

[33] P. J. Steinhardt and F. S. Accetta, Phys. Rev. Lett. **64**, 2740 (1990); J. D. Barrow and K. Maeda, Nucl. Phys. B **341**, 1990 (1990); J. Garcia-Bellido and M. Quiros, Phys. Lett. B **243**, 45 (1990); R. Holman, E. W. Kolb, and Y. Wang, Phys. Rev. Lett. **65**, 17 (1990).

[34] A. D. Linde, Phys. Lett. B **238**, 160 (1990).

[35] Planck: http://astro.estec.esa.nl/Planck.